Electronic Supplementary Material (ESI) for Dalton Transactions.

Supporting information

Structure and Thermal Expansion Behavior of Ca4La6-xNdx(SiO4)4(PO4)2O2 Apatite for Nuclear Waste Immobilization

*Shan Yan, Dongyan Yang, Shuangqiang Chen, Juan Wen, Wenhao He, Shiyin Ji, Yue Xia, Yinlong Wang, Liangfu Zhou, Yuhong Li**

School of Nuclear Science and Technology, Lanzhou University, Lanzhou 730000, China

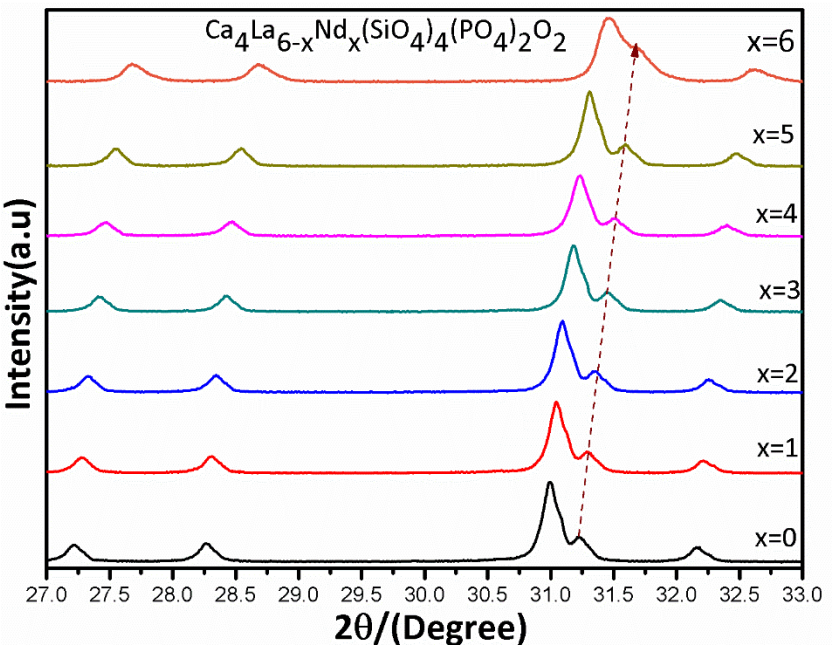

Figure S1. the local graph of powder XRD patterns of $Ca_4La_{6-x}Nd_x(SiO_4)_4(PO_4)_2O_2$ (x=0, 1, 2, 3, 4, 5, 6).

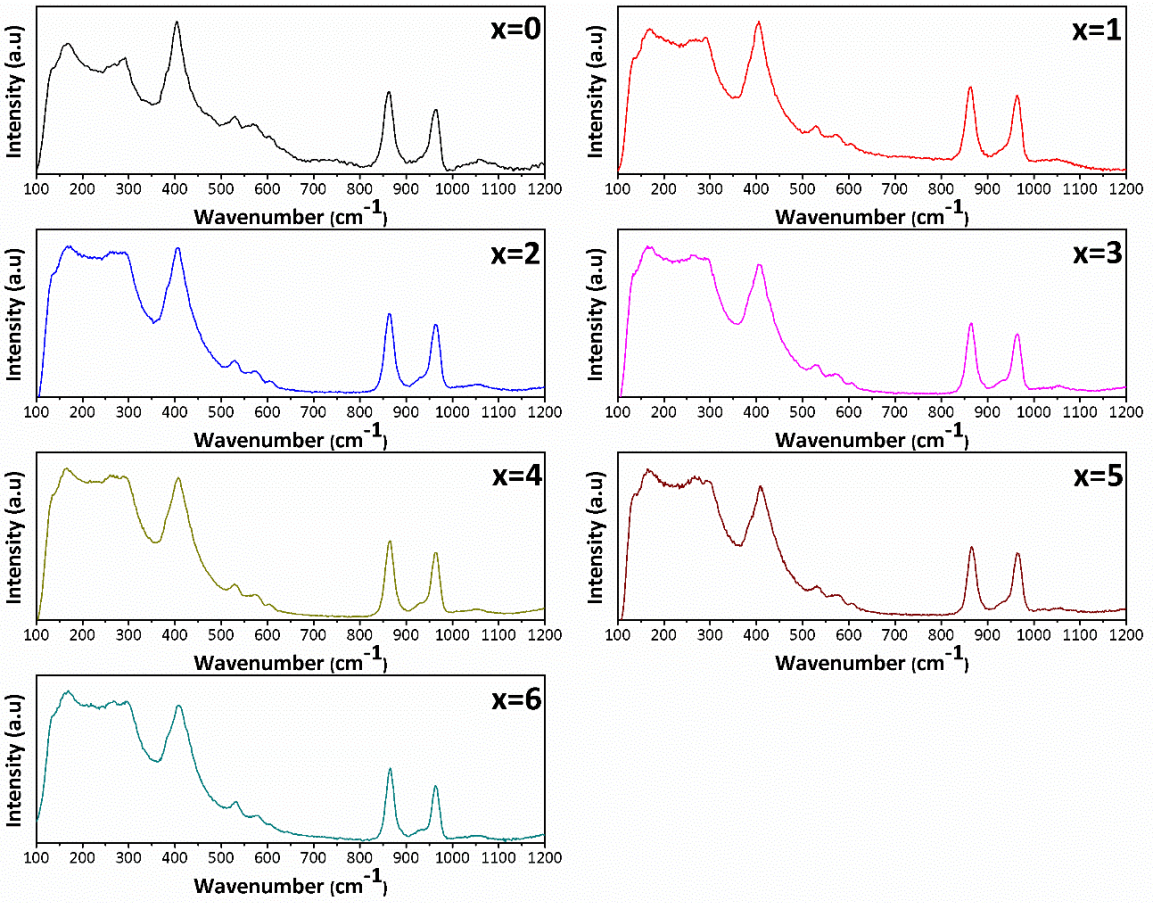

Figure S2. The Raman spectra of $Ca_4La_{6-x}Nd_x(SiO_4)_4(PO_4)_2O_2$ (x = 0, 1, 2, 3, 4, 5, 6) specimens excited in 532 nm.

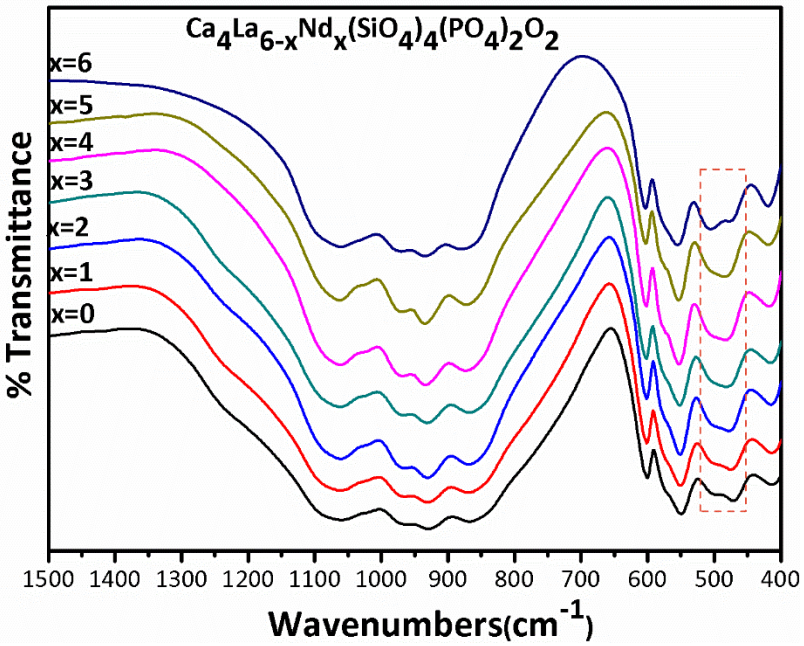

Figure S3. the FT-IR spectra of $Ca_4La_{6-x}Nd_x(SiO_4)_4(PO_4)_2O_2$ (x = 0, 1, 2, 3, 4, 5, 6) samples detected between 400 and 1500 cm^{-1}.

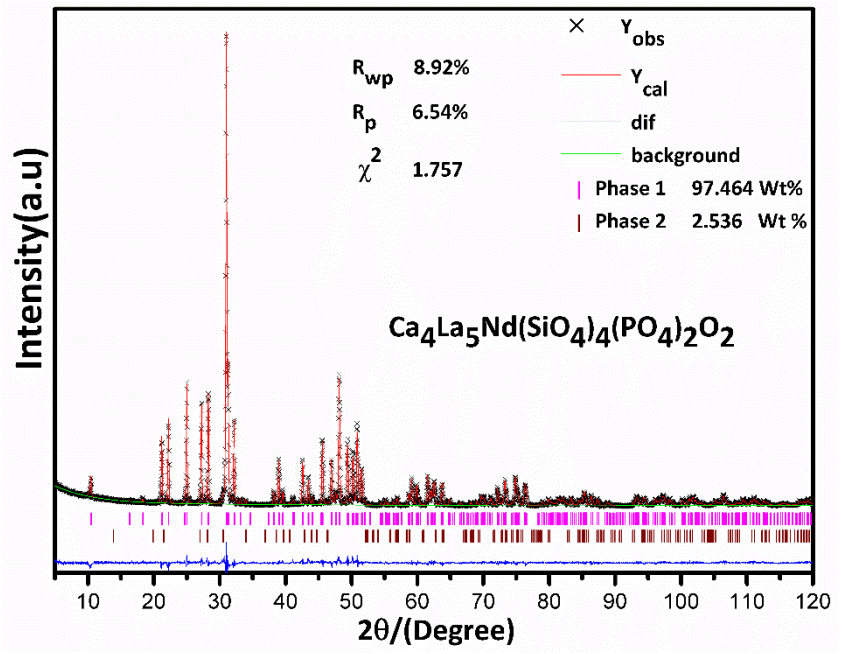

Figure S4. Rietveld fitting pattern for $Ca_4La_5Nd(SiO_4)_4(PO_4)_2O_2$ sample.

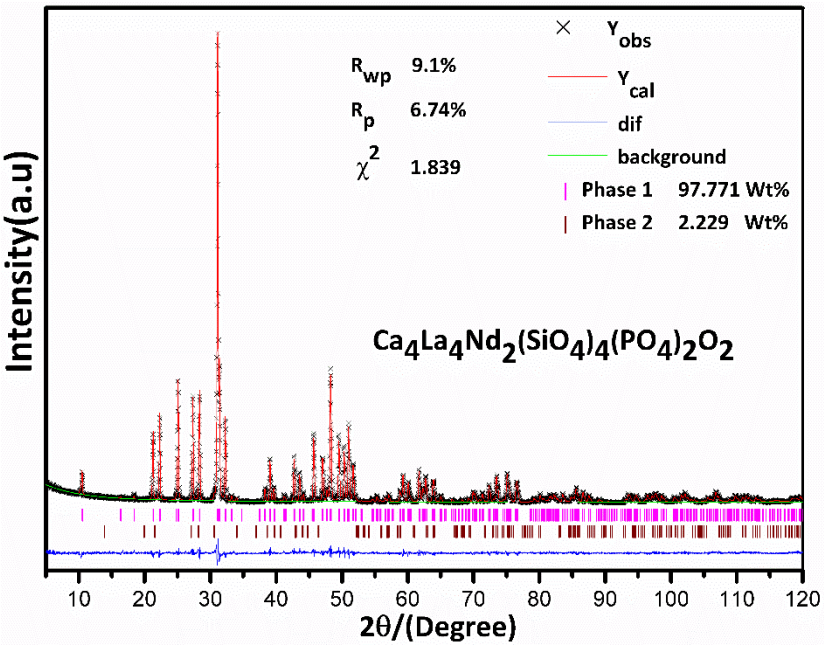

Figure S5. Rietveld fitting pattern for $Ca_4La_4Nd_2(SiO_4)_4(PO_4)_2O_2$ sample.

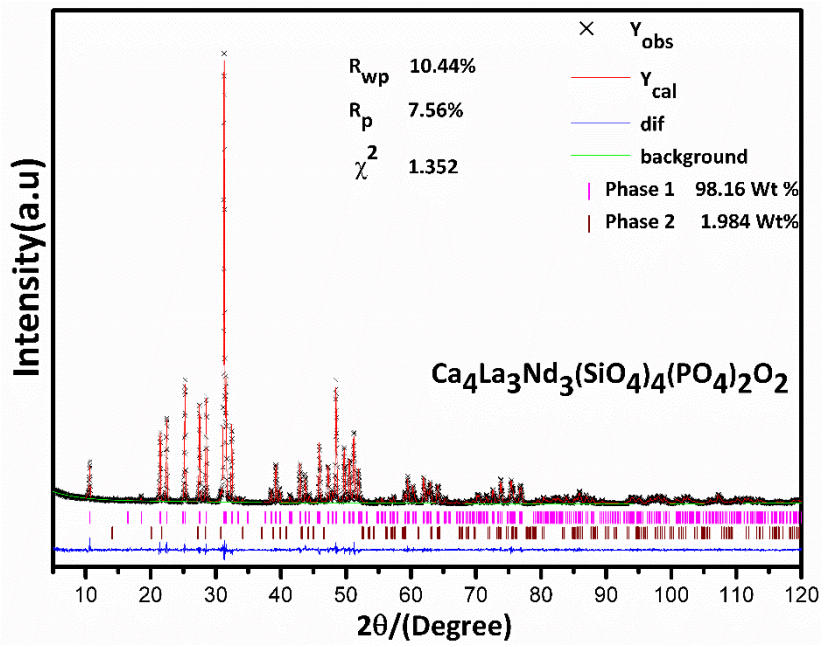

Figure S6. Rietveld fitting pattern for $Ca_4La_3Nd_3(SiO_4)_4(PO_4)_2O_2$ sample.

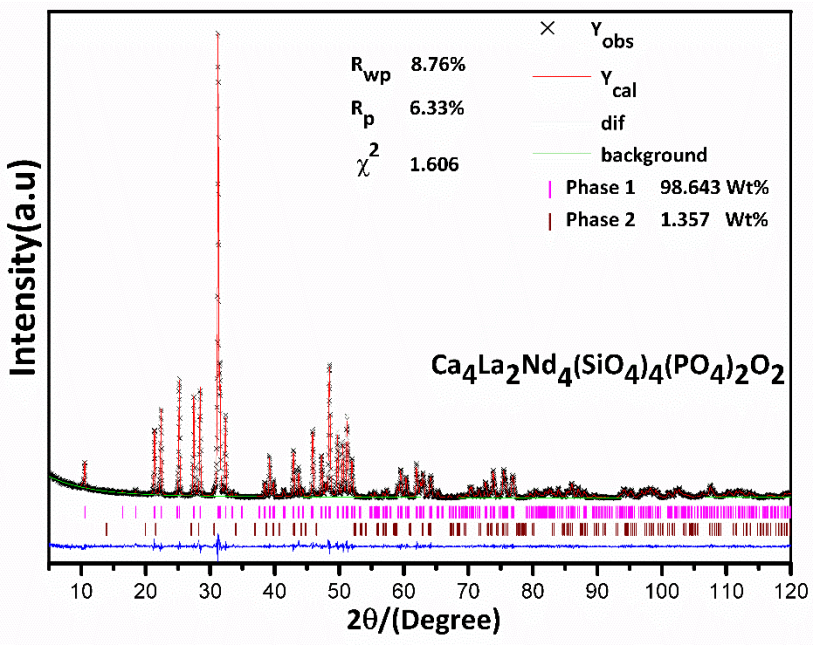

Figure S7. Rietveld fitting pattern for $Ca_4La_2Nd_4(SiO_4)_4(PO_4)_2O_2$ sample.

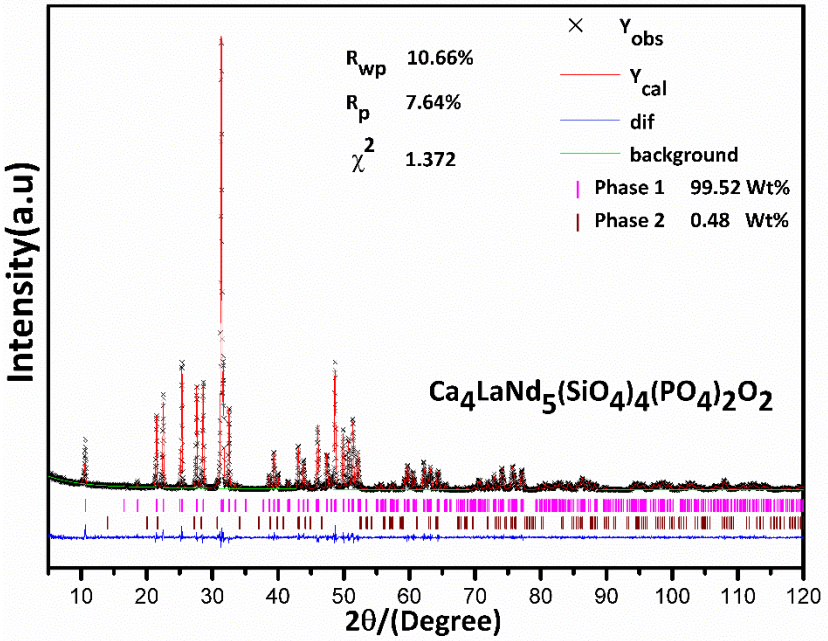

Figure S8. Rietveld fitting pattern for $Ca_4LaNd_5(SiO_4)_4(PO_4)_2O_2$ sample.

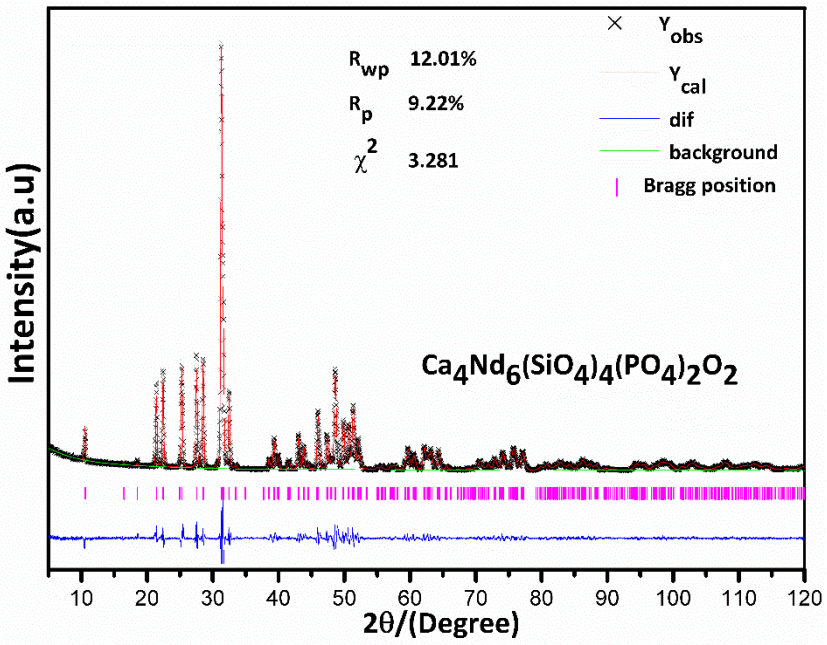

Figure S9. Rietveld fitting pattern for $Ca_4Nd_6(SiO_4)_4(PO_4)_2O_2$ sample.

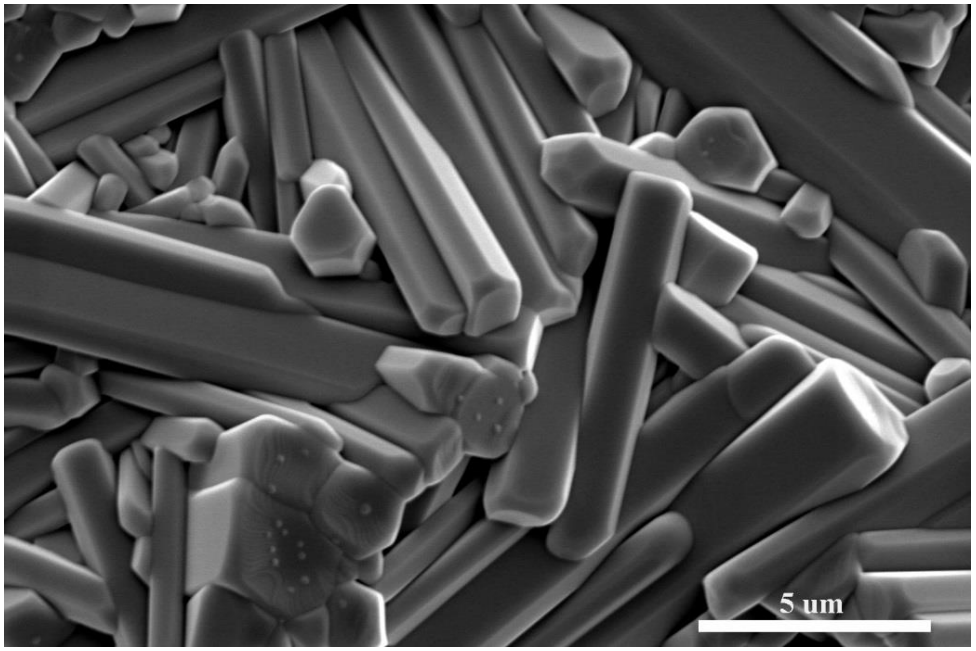

Figure S10. The scanning electron microscope (SEM) of $Ca_4Nd_6(SiO_4)_4(PO_4)_2O_2$ sample prepared at 1600 ℃

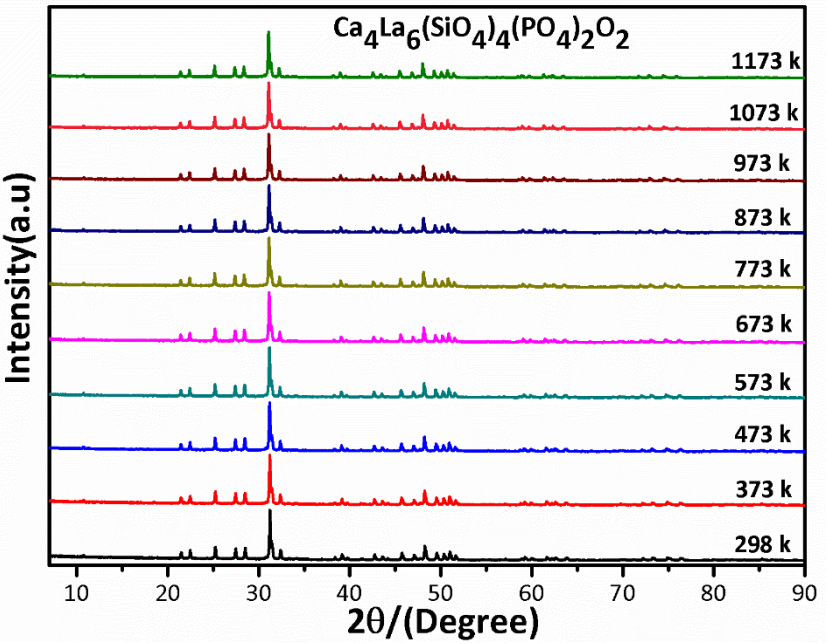

Figure S11. High temperature powder XRD patterns of $Ca_4La_6(SiO_4)_4(PO_4)_2O_2$ sample between 298 and 1173k.

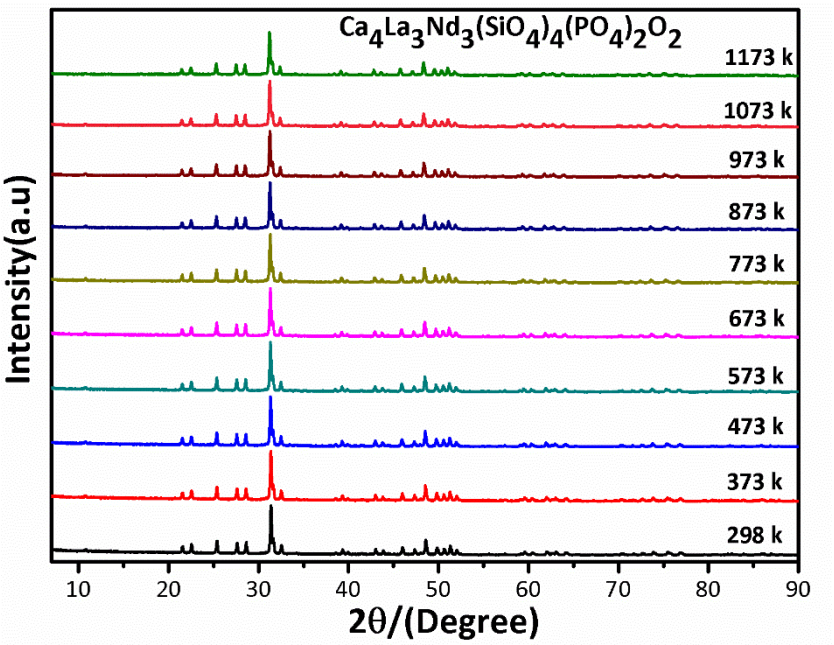

Figure S12. High temperature powder XRD patterns of $Ca_4La_3Nd_3(SiO_4)_4(PO_4)_2O_2$ sample between 298 and 1173k.

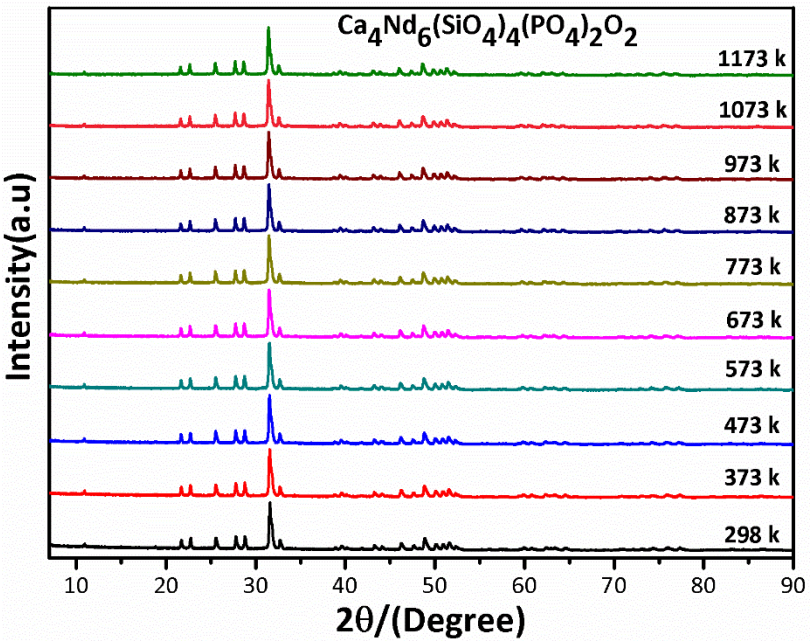

Figure S13. High temperature powder XRD patterns of $Ca_4Nd_6(SiO_4)_4(PO_4)_2O_2$ sample between 298 and 1173k.

Table S1. The refined lattice parameters atomic positions, site occupancy, and isotropic atomic displacement parameters from powder X-ray diffraction of $Ca_4La_{6-x}Nd_x(SiO_4)_4(PO_4)_2O_2$ (x = 0, 1, 2, 3, 4, 5, 6) samples in $P6_3/m$ (176) space group.

Composition x	0	1	2	3	4	5	6
a (Å)	9.5998(1)	9.5815(1)	9.5626(1)	9.5487(1)	9.5278(1)	9.5147(1)	9.5045(2)
c (Å)	7.0886(1)	7.0694(1)	7.0506(1)	7.0373(1)	7.0184(1)	7.0062(1)	6.9983(2)
Volume (Å^3)	565.74(2)	562.06(1)	558.36(1)	555.67(1)	551.76(2)	549.30(2)	547.50(2
R_{wp}	9.04%	8.92%	9.1%	10.44%	8.76%	10.66%	12.01%
R_p	6.65%	6.54%	6.74%	7.56%	6.33%	7.64%	9.22%
χ^2	1.939	1.757	1.839	1.352	1.606	1.372	3.281
M_{4f},4f($^1/_3$,$^2/_3$,z) z	0.003292(1)	0.001697(1)	0.003057(1)	0.001004(1)	0.002190(1)	0.000820(1)	0.003686(1)
Uiso	0.017992(1)	0.018318(1)	0.019203(1)	0.020050(1)	0.019414(1)	0.020839(1)	0.014857(1)
Ca $_{occupy}$	0.76354(3)	0.75911(3)	0.75468(3)	0.75025(3)	0.74582(3)	0.74139(3)	0.73696(3)
La $_{occupy}$	0.23646(3)	0.19705(3)	0.15764(3)	0.11823(3)	0.07882(3)	0.03941(3)	0
Nd $_{occupy}$	0	0.04384(3)	0.08768(3)	0.13152(3)	0.17536(3)	0.21920(3)	0.26304(3)
M_{6h},6h(x, y, $^1/_4$) x	0.246351(1)	0.245815(1)	0.245105(1)	0.244026(1)	0.243715(1)	0.242948(1)	0.243114(1)
M_{6h},6h(x, y, $^1/_4$) y	0.230990(1)	0.231276(1)	0.231132(1)	0.230595(1)	0.231058(1)	0.230562(1)	0.231605(1)
Uiso	0.011804(1)	0.012316(1)	0.011576(1)	0.012457(1)	0.010411(1)	0.012617(1)	0.014452(1)
Ca $_{occupy}$	0.15764(2)	0.16059(2)	0.16355(2)	0.16650(2)	0.16945(2)	0.17241(2)	0.17536(2)
La $_{occupy}$	0.84236(2)	0.70196(2)	0.56157(2)	0.42118(2)	0.28079(2)	0.14039(2)	0
Nd $_{occupy}$	0	0.13744(2)	0.27488(2)	0.41232(2)	0.54976(2)	0.68720(2)	0.82464(2)
Si/P,6h(x, y, $^1/_4$) x	0.028670(1)	0.030225(1)	0.028133(1)	0.030759(1)	0.029600(1)	0.031077(1)	0.030626(1)
Si/P,6h(x, y, $^1/_4$) y	0.4077520(1)	0.406969(1)	0.406043(1)	0.402822(1)	0.404972(1)	0.402400(1)	0.403019(1)
Uiso	0.015018(1)	0.015346(1)	0.015936(1)	0.018515(1)	0.015704(1)	0.016746(1)	0.018997(1)
O1, 6h(x, y, $^1/_4$) x	0.492079(1)	0.494547(1)	0.489717(1)	0.494914(1)	0.492930(1)	0.491165(1)	0.492332(1)
O1, 6h(x, y, $^1/_4$) y	0.156819(1)	0.154608(1)	0.157917(1)	0.152915(1)	0.154915(1)	0.152905(1)	0.153181(1)
Uiso	0.000280(1)	0.008125(1)	0.007301(1)	0.013631(1)	0.006791(1)	0.010966(1)	0.015623(1)
O2, 6h(x, y, $^1/_4$) x	0.139030(1)	0.135223(1)	0.133189(1)	0.128848(1)	0.131162(1)	0.124961(1)	0.126440(1)
O2, 6h(x, y, $^1/_4$) y	0.598758(1)	0.598713(1)	0.598190(1)	0.595574(1)	0.598032(1)	0.595869(1)	0.596669(1)
Uiso	0.015816(1)	0.013862(1)	0.012678(1)	0.022898(1)	0.015693(1)	0.016448(1)	0.017732(1)
O3, 12i(x, y, z) x	0.085774(1)	0.085489(1)	0.085412(1)	0.086625(1)	0.086359(1)	0.086085(1)	0.089737(1)
O3, 12i(x, y, z) y	0.345350(1)	0.342600(1)	0.341289(1)	0.337316(1)	0.341053(1)	0.336099(1)	0.342431(1)
O3, 12i(x, y, z) z	0.070677(1)	0.070502(1)	0.071902(1)	0.070801(1)	0.069409(1)	0.069565(1)	0.067906(1)
Uiso	0.014541(1)	0.006960(1)	0.018439(1)	0.018331(1)	0.008517(1)	0.018893(1)	0.016092(1)
O4, 2a(0, 0, $^1/_4$)							
Uiso	0.023588(1)	0.020444(1)	0.015745(1)	0.015242(1)	0.017955(1)	0.016307(1)	0.017937(1)

Table S2. The selected bond lengths and Bond-Valence Sums (BVS) of $Ca_4La_{6-x}Nd_x(SiO_4)_4(PO_4)_2O_2$ (x = 0, 1, 2, 3, 4, 5, 6) samples after refinement analyses.

Composition x	0	1	2	3	4	5	6
Si/P — O(1)	1.5543(1)	1.5529(1)	1.5512(1)	1.5475(1)	1.5415(1)	1.5390(1)	1.5362(1)
Si/P — O(2)	1.5944(1)	1.5935(1)	1.5936(1)	1.5940(1)	1.5937(1)	1.5944(1)	1.5940(1
Si/P — O(3)*2	1.6136(1)	1.6117(1)	1.6123(1)	1.6124(1)	1.6122(1)	1.6125(1)	1.6108(1)
<Si/P — O >	1.593975	1.59245	1.59235	1.591575	1.5899	1.5896	1.58795
M_{4f}— O(1) *3	2.4625(3)	2.4483(3)	2.4540(4)	2.4397(3)	2.4389(4)	2.4407(4)	2.4478(4)
M_{4f}— O(2)*3	2.3972(3)	2.4233(3)	2.4228(3)	2.4532(3)	2.4297(3)	2.4692(3)	2.4439(3)
M_{4f}— O(3)*3	2.8390(4)	2.8539(2)	2.8567(5)	2.8759(3)	2.8430(4)	2.8739(4)	2.8149(5)
< M_{4f}— O >	2.566233	2.575167	2.577833	2.5896	2.570533	2.5946	2.568867
M_{6h} — O(1)	2.7841(1)	2.8231(1)	2.7567(1)	2.8401(1)	2.8084(1)	2.8051(1)	2.8164(1)
M_{6h} — O(2)	2.5713(1)	2.5329(1)	2.5168(1)	2.5045(1)	2.4934(1)	2.4625(1)	2.4565(1)
M_{6h} — O(3)*2	2.6248(1)	2.5974(1)	2.5743(1)	2.5336(1)	2.5542(1)	2.5165(1)	2.5287(1)
M_{6h} — O(3)*2	2.4259(1)	2.4136(1)	2.4157(1)	2.3992(1)	2.3932(1)	2.3890(1)	2.3858(1)
M_{6h} — O(4)	2.2948(1)	2.2888(1)	2.2800(1)	2.2687(1)	2.2642(1)	2.2550(1)	2.2580(1)
< M_{6h} — O >	2.535942	2.523829	2.504786	2.496986	2.4944	2.476229	2.479986
Ca_{4f} BVS	2.00812	1.96402	1.95068	1.89934	1.97778	1.86464	1.94776
La_{4f} BVS	3.36448	3.3035	3.28484	3.21181	3.32448	3.16517	
Nd_{4f} BVS		2.94585	2.92585	2.84884	2.96649	2.79679	2.92146
Ca_{6h} BVS	1.63415	1.69683	1.75604	1.8252	1.83308	1.93144	1.90576
La_{6h} BVS	2.72459	2.80975	2.89601	2.98483	2.99552	3.12917	
Nd_{6h} BVS		2.5451	2.6369	2.73764	2.74946	2.89699	2.85848

Table S3. The crystal data, thermal expansion coefficients and anisotropic parameters (α_a/α_c) of $Ca_4La_6(SiO_4)_4(PO_4)_2O_2$ material in the temperature range of 298-1173 K.

T(K)	a (Å)	$\alpha_a \cdot 1x10^6(K^{-1})$	c (Å)	$\alpha_c \cdot 1x10^6(K^{-1})$	α_a/α_c	V(Å^3)	$\alpha_v \cdot 1x10^6(K^{-1})$
			$Ca_4La_6(PO_4)_4(SiO_4)_2O_2$				
298	9.595942	9.017287	7.086222	6.990531	1.289929	565.094	25.05781
373	9.60277	8.778117	7.090028	6.8225961	1.286624	566.202	24.42984
473	9.610834	8.459224	7.094772	6.598684	1.281956	567.533	23.59255
573	9.618629	8.140331	7.099213	6.374771	1.27696	568.81	22.75526
673	9.626481	7.821438	7.104156	6.150859	1.271601	570.136	21.91797
773	9.634238	7.502544	7.108468	5.926946	1.265836	571.402	21.08068
873	9.640447	7.183651	7.111515	5.703033	1.259619	572.383	20.24339
973	9.647381	6.864758	7.11611	5.479121	1.252894	573.578	19.4061
1073	9.654068	6.545865	7.119841	5.255208	1.245596	574.674	18.56881
1173	9.660237	6.226972	7.123816	5.031296	1.237648	575.73	17.73152

Table S4. The crystal data, thermal expansion coefficients and anisotropic parameters (α_a/α_c) of $Ca_4La_3Nd_3(SiO_4)_4(PO_4)_2O_2$ material in the temperature range of 298-1173 K.

T(K)	a (Å)	α_a·1x10^6(K^{-1})	c (Å)	α_c·1x10^6(K^{-1})	α_a/α_c	V(Å^3)	α_v· 1x10^6(K^{-1})
$Ca_4La_3Nd_3(PO_4)_4(SiO_4)_2O_2$							
298	9.539958	8.414846	7.030376	6.901902	1.219207	554.118	23.756346
373	9.546563	8.240396	7.034348	6.766088	1.217897	555.199	23.290260
473	9.553801	8.007795	7.038675	6.585003	1.216066	556.383	22.668811
573	9.561501	7.775195	7.043566	6.403918	1.214131	557.668	22.047362
673	9.569093	7.542594	7.048214	6.222832	1.212084	558.922	21.4259132
773	9.5753	7.309993	7.051809	6.041747	1.209914	559.933	20.8044642
873	9.583012	7.077393	7.056283	5.860662	1.20761	561.191	20.1830152
973	9.589323	6.844792	7.060413	5.679576	1.205159	562.259	19.561567
1073	9.5956	6.612192	7.064185	5.498491	1.202547	563.296	18.940118
1173	9.60211	6.379591	7.068286	5.317406	1.199756	564.388	18.318669

Table S5. The crystal data, thermal expansion coefficients and anisotropic parameters (α_a/α_c) of $Ca_4Nd_6(SiO_4)_4(PO_4)_2O_2$ material in the temperature range of 298-1173 K.

T(K)	a (Å)	$\alpha_a \cdot 1x10^6(K^{-1})$	c (Å)	$\alpha_c \cdot 1x10^6(K^{-1})$	α_a/α_c	V(Å^3)	$\alpha_v \cdot 1x10^6(K^{-1})$
$Ca_4Nd_6(PO_4)_4(SiO_4)_2O_2$							
298	9.50071	8.75291	6.998637	6.661747	1.313906	547.087	24.18698
373	9.508645	8.448338	7.003143	6.438064	1.312248	548.354	23.36922
473	9.515563	8.042243	7.007056	6.13982	1.30985	549.459	22.27887
573	9.523204	7.636147	7.011481	5.841576	1.307207	550.689	21.18852
673	9.530037	7.230051	7.015135	5.543332	1.304279	551.767	20.09817
773	9.537024	6.823955	7.018915	5.245089	1.301018	552.874	19.00782
873	9.543005	6.417859	7.022811	4.946845	1.297364	553.875	17.91747
973	9.548056	6.011763	7.0254	4.648601	1.293241	554.666	16.82712
1073	9.55421	5.605667	7.028605	4.350357	1.288553	555.635	15.73677
1173	9.560196	5.199571	7.032516	4.052113	1.283175	556.641	14.64642